CHAPTER 4

Development of P(NIPAAm-*co*-MBA) Hydrogels

Part of work published in EXPRESS Polymer Letters

4.1 Introduction

Poly-*N*-isopropylacrylamide (PNIPAAm) is one of the most extensively studied thermoresponsive polymer in the literature due to its remarkable volumetric phase transition properties. PNIPAAm rapidly and reversibly switches between the hydrophobic and hydrophilic states at temperatures above and below the lower critical solution temperature (LCST) (~32 °C) respectively. The main driving force for the LCST of PNIPAAm is said to be entropy of the system due to water-water interactions above the LCST. PNIPAAm is particularly attractive for biological applications, since the polymer is water-soluble, it is biocompatible, and the phase transition can be easily triggered between ambient temperature and body temperature. This unique behaviour has attracted widespread attention and many applications of PNIPAAm are being investigated which include thermo-responsive membranes, reversible immobilization of bio macromolecules, *in vitro* cell culture, separation of molecules from aqueous mixtures, and drug delivery.

Despite the favourable properties of PNIPAAm these smart polymeric hydrogels display two major limitations, i.e. poor mechanical properties and slow response time to temperature changes (Zhang et al., 2008). The slow response rate of monolithic PNIPAAm hydrogels to temperature is believed to be due to the formation of a dense skin layer which forms as a result of the strong hydrophobic interactions existing among the isopropyl groups in the PNIPAAm molecule, which retards the outward diffusion of water molecules above the LCST. Additionally, the swelling rate of the hydrogel at the temperatures below LCST is even slower (Zhang et al., 2008). Bulk PNIPAAm hydrogels may not be applicable for a range of practical applications where more robust response are required such as in cell-culture, drug delivery, and on-off switches.

The focus of many studies in recent years has therefore been on improving the mechanical properties and response rate of PNIPAAm hydrogels. Some of the strategies which are being investigated include cross-linking; synthesis of a heterogeneous hydrogel structure using mixed solvents; the use of porogens (e.g. polyethylene glycol); the use of hydrophilic co-polymers to increase hydrogen bonding; and cold polymerisation (to create a porous structure) amongst others (Zhang et al., 2008).

Chemical cross-linking is one of the simplest and most versatile tools for controlling the mechanical properties and response rate of hydrogels (Geever et al., 2007). It is well-known that chemical cross-linking can be used to increase the mechanical stability of hydrogels (Geever et al., 2007). However excessive cross-linking may compromise the swelling properties and open interconnected structures of hydrogels (Caykara et al., 2006a). Hence an optimum level of cross-linking is desired to achieve good mechanical properties and a fast response while also maintaining the LCST of the hydrogel.

The most common method for synthesising PNIPAAm hydrogels is by copolymerising NIPAAm with N,N'-methylenebisacrylamide (MBA) to produce P(NIPAAm-*co*-N,N'-methylenebisacrylamide) (P(NIPAAm-*co*-MBA)). MBA serves as the cross-linker, and ammonium persulphate (APS) and N,N,N',N'-tetramethylethylenediamine (TEMED) are commonly used the redox initiator pair.

In this study the cross-link density (R) of the hydrogels is expressed as a molar ratio of monomer to cross-linker as follows:

$$R = \frac{nMoles\ monomer}{nMoles\ crosslinker} \qquad \text{(Eq 4.1)}$$

In the literature, various cross-link densities have been reported for P(NIPAAm-*co*-MBA) hydrogels. However cross-link densities investigated have typically being rather low ranging between R 500-50 (i.e. < 2 Mol% MBA) (Caykara et al., 2006b; DeRosa et al., 2007; Liang et al., 2000; Zhang et al., 2002b). It is known that for a number of applications PNIPAAm hydrogels with improved stability and mechanical strength are required.

Also the viscoelastic behaviour of PNIPAAm hydrogels has not been widely reported. Mechanical properties of PNIPAAm and other hydrogels have typically being investigated under stress-strain or tension/compression studies (Muniz and Geuskens, 2001; Takigawa et al., 1997). Rheology however has not been widely investigated for PNIPAAm hydrogels. Rheology provides information about the strength, relaxation and viscoelastic properties of gels, while providing a very accurate determination of the LCST.

In this study P(NIPAAm-*co*-MBA) hydrogels were synthesised for assessment of its physical and mechanical properties. The cross-link density of the hydrogels was varied from R 90-10 (1.1-9.1 MBA Mol%) and the use of mixed solvent : water systems were investigated as the co-polymerisation medium. The LCST, swelling, de-swelling behaviour, morphology, contact angle and viscoelastic properties of the P(NIPAAm-*co*-MBA) hydrogels are reported.

4.2   Experimental

4.2.1 Materials

N-isopropylacrylamide (NIPAAm, 97% purity), N,N'-methylenebisacrylamide (MBA, 99% purity) and ammonium persulphate (APS >98%, ACS reagent) were obtained from Sigma Aldrich and used as received. N,N,N',N'-tetramethylethylenediamine (TEMED) was obtained from Merck. High purity analytical grade tetrahydrofuran and acetone were used. Water was purified by the use of reverse osmosis UV ultra-purification water system.

### 4.2.2 Synthesis of P(NIPAAm-*co*-MBA) hydrogels

4.2.2.1 Preparation of standard P(NIPAAm-*co*-MBA) hydrogels

P(NIPAAm-*co*-MBA) hydrogels were synthesised by *in situ* free radical polymerisation of NIPAAm using MBA as the cross-linker agent, and APS and TEMED as the redox initiators as shown in **Scheme 4.1** (Zhang et al., 2003). A 10% (w/v) aqueous stock solution of NIPAAm was prepared by dissolving 10 g of NIPAAm in 100 ml of water in a volumetric flask with magnetic stirring. A 10 wt% APS solution was freshly prepared by dissolving 1 g of APS in 10 ml of deionised water. For the standard formulation (R 90), 1.5 wt% MBA in the monomer feed, and 2 wt% each APS and TEMED, was used based on the NIPAAm mass.

Briefly 10 ml of the 10 wt% NIPAAm solution was pipetted into a glass reaction vessel. 0.015 g of MBA was added to the mixture and stirred until dissolved. Thereafter 25.8 µl of TEMED was added and stirred until homogenised. The vessel was then inserted in an ice-bath at 5 ℃ and the solution was left to pre-cool for 5 minutes. The APS solution was also placed in the ice-bath to cool. Thereafter 200 µl of a pre-cooled 10% (w/v) APS solution was added to the NIPAAm solution to initiate

polymerisation. Polymerisation was conducted at 5 °C for 30 minutes and thereafter the solution was left to polymerise at ambient temperature of 23 °C for 24 hours.
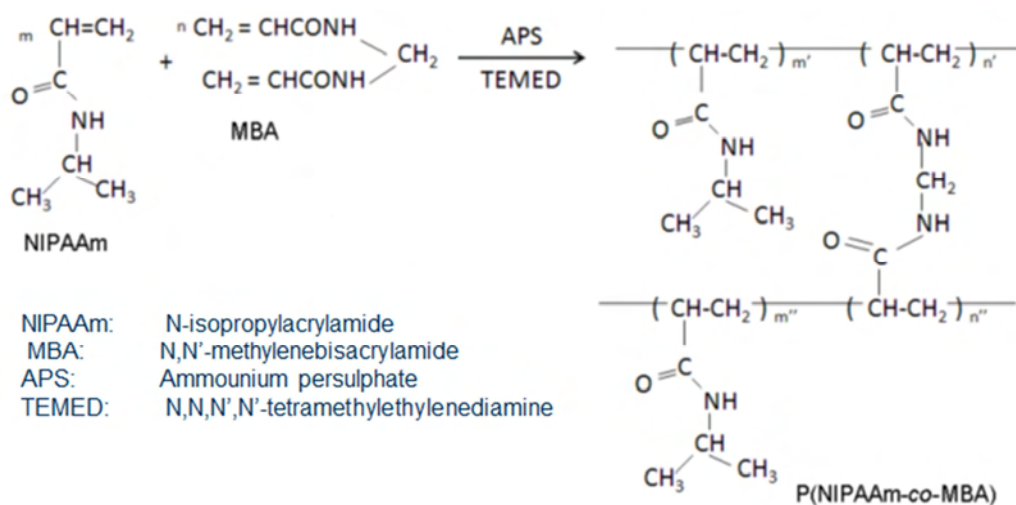
Scheme 4.1: Synthesis scheme of PNIPAAm hydrogels by free radical polymerisation using MBA as the cross-linker and APS and TEMED as the redox initiators (where m = m' + m'' and refers to the NIPAAm units, while n= n' +n'' and refers to the MBA units) (Zhang et al., 2003).

After polymerisation, the hydrogels were leached in cold deionised water for several days to remove any unreacted monomers. Residual contaminants in the water washes were monitored from 190-250 nm using a UV-VIS spectrophotometer.

4.2.2.2   Varying cross-link density

P(NIPAAm-*co*-MBA) hydrogels were prepared as detailed above, except the cross-link density was varied between R 90-10. R was determined as the molar ratio of NIPAAm to MBA. The feed composition of the P(NIPAAm-*co*-MBA) hydrogels is given in **Table 4.1**.

4.2.2.3 Use of mixed solvents

To increase porosity and improve the swelling rate of the P(NIPAAm-*co*-MBA) gels, mixed solvent systems were used as the co-polymerisation medium. The hydrogels were prepared as described in **Section 4.2.2.1** but instead of using water, acetone:water and tetrahydrofuran (THF) : water mixtures were used (Zhang et al., 2002a; Zhang et al., 2002b) (**Table 4.2**).

Table 4.1:   Feed composition of cross-linked P(NIPAAm-*co*-MBA) hydrogels.

Gel No.	R	NIPAAm Mol %	MBA Mol %	MBA wt % in the monomer feed
1*	90	98.9	1.1	1.5
2	70	98.6	1.4	1.9
3	50	98.0	2.0	2.7
4	30	96.8	3.2	4.3
5	10	90.9	9.1	12.0

(*Gel 1 represents the standard formulation)

Table 4.2:   Solvent:water mixtures used during co-polymerisation with R 90.

Gel No.	Solvent	Solvent : water Vol%
6	Acetone	30:70
7	Acetone	50:50
8	THF	30:70
9	THF	50:50

4.2.3 Characterisation of P(NIPAAm-*co*-MBA) hydrogels

4.2.3.1 Differential scanning calorimetry

A Perkin Elmer Differential Scanning Calorimeter (DSC 7) was used to determine the LCST of the PNIPAAm hydrogels. The cross-linked gels were swollen in water to equilibrium prior to analysis. The temperature range analysed was 5 to 60 ℃ using a scan rate of 5 ℃/min, with a nitrogen purge rate o f 40 ml/min. The LCST was taken at the onset to the peak maximum.

4.2.3.2 Swelling

After polymerisation, hydrogels were carefully cut into 1.5 cm disks. The equilibrium gravimetric swelling ratios of the hydrogels were determined by equilibrating the gel pieces in deionised water at room temperature (20 ºC) for 24 hours. The swelling ratios (SR) of the P(NIPAAm-*co*-MBA) gels were calculated as follows:

$$\text{Swelling ratio} = \frac{W_w - W_d}{W_d} \qquad\qquad \text{(Eq. 4.2)}$$

where Ww is the wet weight of the gel and Wd is the weight of the xerogel (dried gel). When measuring the wet weight of the gels, gel pieces were gently placed between two filter papers to remove the excess surface water, and the wet gels were weighed. Deswelling kinetics of the gels was performed gravimetrically by placing fully swollen gels in the oven at 37 ºC. Gels were weighed at following time intervals i.e. 0, 10, 20, 30, 45, 60, and 90 minutes. The percent water retention was determined as follows:

$$\% \text{ water uptake or } \% \text{ water retention} = \frac{W_w - W_d}{W_s - W_d} * 100 \qquad \text{(Eq. 4.3)}$$

Where W_s is the weight of the fully swollen gel.

4.2.3.3 Environmental scanning electron microscopy (ESEM)

ESEM analysis was conducted by Prof Burton at the Centre for Electron Microscopy at the University of Kwazulu Natal in Pietermaritzburg. Analysis involved incubating polymerised gels in water at ambient temperature until fully equilibrated. Samples were then imaged using an environmental scanning electron microscope without any sample preparation. When samples were viewed at 25 ℃, a CP+ aperture holder under low vacuum mode with LFD at 1 torr. At 37 ℃, best images were obtained under wet mode - using a peltier cooling stage with a GSED and a pressure of 4 torr, and relative humidity ~ 8%.

4.2.3.4 Analysis of viscoelastic properties

For determination of the viscoelastic properties of the hydrogels, an Anton Paar UDS 200 rheometer was used with a plate-plate arrangement. The analysis was performed at the Department of Physical Chemistry and Material Science at the Budapest University of Technology and Economics. Shear strain was applied between two parallel plates which were 0.5 mm apart. The dry gel samples were applied to the plate, deionised water was added, and equilibrium swelling was attained. Excess water was wiped with a tissue paper and after the sample thickness was adjusted, excess water was again added to the plate to avoid the loss of water from the sample during the measurements. The average of three samples was taken for each measurement. To determine the linear viscoelastic region a strain of 0.01 −

100% at 10 s^{-1} angular frequency (ω) was applied at 25 ℃. Temperature and frequency sweeps were conducted to obtain the storage modulus (G′), loss modulus (G″), and damping factor (tan δ) of the P(NIPAAm-*co*-MBA) hydrogels. Temperature sweeps were carried out at 25-60 ℃ at 3 ℃/min hea ting rate at 10 s^{-1} ω and 1% strain, while the frequency sweeps were conducted at 25 ℃ and 60 ℃ with ω of 1-100 s^{-1} at 1% strain.

4.2.3.5 Water contact angle

The water contact angle of the PNIPAAm gels (gels 1-5) were measured with a Krüss DSA100 tensiometer. Contact angle measurements were taken at 20 °C, and at 40 °C at 5 second intervals over a 65 second period. Gels were equilibrated in the sample chamber for 30 minutes at the respective temperature prior to analysis. Equilibrated gels were cut into 1x1 cm dimensions, gently wiped with tissue paper to remove excess surface water, and were placed on a stage in a temperature – controlled chamber. A real-time image of the gels was obtained with the Krüss Drop Shape analysis software using the sessile drop type. At each temperature point five analyses were performed.

4.3 Results & discussion

In this study the physical properties of P(NIPAAm-*co*-MBA) hydrogels were investigated by varying the cross-link density of the hydrogels, and by evaluating the use of solvent mixtures as the co-polymerisation medium. The following results will be discussed i.e. mechanism of free radical polymerisation (**Section 4.3.1**); assessment of gel formulations (**Section 4.3.2**); LCST by DSC (**Section 4.3.3**); morphology (**Section 4.3.4**); swelling and de-swelling properties (**Section 4.3.5**), viscoelastic properties (**Section 4.3.6**); and water contact angle (**Section 4.3.7**).
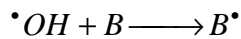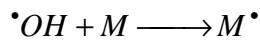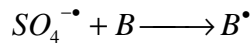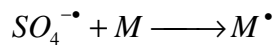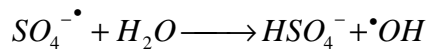
4.3.1 Mechanism for free radical polymerisation

Free radical polymerisation of PNIPAAm hydrogels proceeds via addition polymerisation across the double bond of the vinyl group of the NIPAAm monomer. MBA was used as the cross-linking agent, and APS and TEMED was the redox initiator pair where APS acts as the oxidiser and TEMED is the reducing agent. The
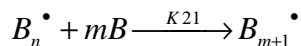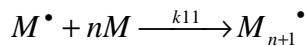
reaction mechanism for the formation of P(NIPAAm-*co*-MBA) is given in **Scheme 4.2.** APS decomposes in the presence of TEMED to produce two free radical species i.e. sulphate ($SO_4^{-\bullet}$) radical ions and hydroxyl ($OH^\bullet$) radicals, both of which are capable of initiating polymerisation (Riggs and Rodriguez, 1967). Initiation involves reaction of $SO_4^{-\bullet}$ and $OH^\bullet$ free radicals with the NIPAAm monomer (M) and MBA monomer (B) thereby creating the NIPAAm radical ($M^\bullet$) and MBA radical ($B^\bullet$) respectively.
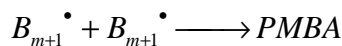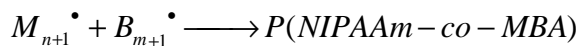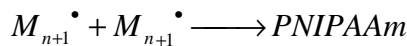
$$Initiation:$$

$$S_2O_8^{2-} \xrightarrow{\ TEMED\ } 2SO_4^{-\bullet}$$

$$SO_4^{-\bullet} + H_2O \longrightarrow HSO_4^{-} + {}^\bullet OH$$

$$SO_4^{-\bullet} + M \longrightarrow M^\bullet$$

$$SO_4^{-\bullet} + B \longrightarrow B^\bullet$$

$${}^\bullet OH + M \longrightarrow M^\bullet$$

$${}^\bullet OH + B \longrightarrow B^\bullet$$

$$\Pr opagation:$$

$$M^\bullet + nM \xrightarrow{\ k11\ } M_{n+1}{}^\bullet$$

$$B_n{}^\bullet + mB \xrightarrow{\ K21\ } B_{m+1}{}^\bullet$$

$$Ter\min ation:$$

$$M_{n+1}{}^\bullet + M_{n+1}{}^\bullet \longrightarrow PNIPAAm$$

$$M_{n+1}{}^\bullet + B_{m+1}{}^\bullet \longrightarrow P(NIPAAm-co-MBA)$$

$$B_{m+1}{}^\bullet + B_{m+1}{}^\bullet \longrightarrow PMBA$$

Scheme 4.2: Mechanism for the synthesis of P(NIPAAm-*co*-MBA) using free-radical polymerisation.

MBA is a very effective cross-linker since it contains two unsaturated bonds in its structure as shown in **Scheme 4.3** which are susceptible to free radical addition. Chain propagation then pursues whereby the NIPAAm radical attacks another NIPAAm monomer to form a growing NIPAAm macroradical ($M_{n+1}\bullet$). Similarly the MBA radical attacks further MBA monomers to create the MBA macroradical ($B_{n+1}\bullet$). This involves a head-to-tail arrangement (i.e. C2 of NIPAAm radical attaches to C1 of NIPAAm monomer, and C2 or C8 of the MBA radical adds to either C1 or C9 of the MBA monomer). Finally termination occurs when two monomer macroradicals interact to form the stable polymer.
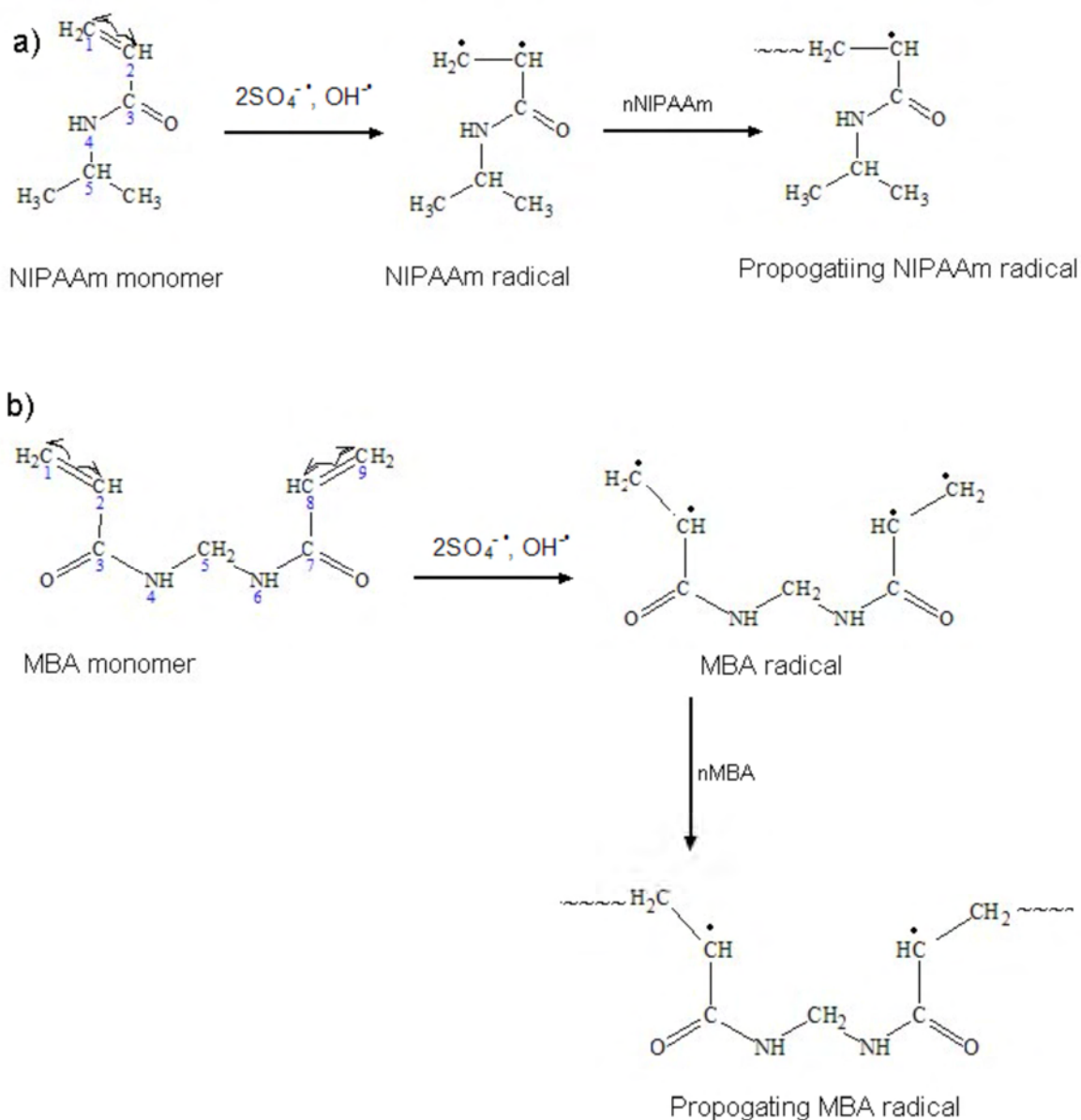
Scheme 4.3: Initiation of a) NIPAAm and b) MBA monomers using APS/TEMED.

In addition to P(NIPAAm-*co*-MBA), PNIPAAm and Poly-N,N'-methylenebisacrylamide (PMBA) can also form as shown in **Scheme 4.2**. The PNIPAAm and PMBA homopolymers were removed by washing the hydrogel in water. The composition of the forming copolymer changes in every picosecond which is known as composition drift. The composition of the final polymer can be determined by the rate constants of the respective reactions, however this was not considered in this study since it was not the subject of this investigation.

4.3.2 Assessment of gel formulations

When water was used as the co-polymerisation medium, P(NIPAAm-*co*-MBA) hydrogels with R 90-30 appeared clear and transparent (**Figure 4.1).** However when the cross-linker content was increased to 9.1 Mol% MBA (R 10), the gel underwent syneresis and appeared opaque following polymerisation.
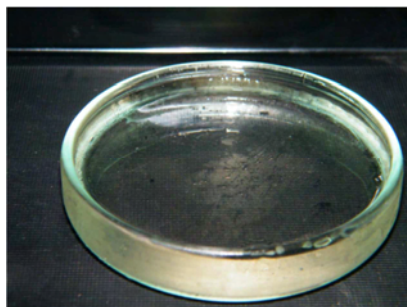
.

Figure 4.1:   Optical image of standard R 90 P(NIPAAm-co-MBA) hydrogel produced by co- polymerisation of NIPAAm and MBA.

It has previously been reported that an increasing cross-linker content increases the degree of inhomogeneities in PNIPAAm hydrogels (Kara et al., 2002). The phase separation in the R 10 gel can be associated with the higher cross-linker content which enhances the reactivity of the reaction. The MBA cross-linker is tetrafunctional and displays a reactivity at least twice that of the NIPAAm due to the presence of two vinyl groups in its structure compared to only one for NIPAAm. The higher rate of reaction for the R 10 gels compared to the R 90-30 gels can result in two plausible effects. Firstly the higher MBA content can result in non-homogenous cross-linking thus resulting in a combination of lightly cross-linked and highly cross-linked domains which results in phase separation of the latter. Secondly the higher MBA content in the R 10 gel can induce a higher heat of polymerisation, resulting in the temperature exceeding the LCST of PNIPAAm during polymerisation, which thereby induces phase separation. This effect however still requires further investigation.Interestingly for both solvent systems the gels were not "transparent" as observed for the standard gel. The 30:70 acetone: water gel, 30:70 THF: water, and 50:50 THF: water gels appeared translucent while the 50:50 acetone: water gel was opaque (**Figure 4.2)**. A summary of the appearance of hydrogels 1-9 appear in **Table 4.3**.
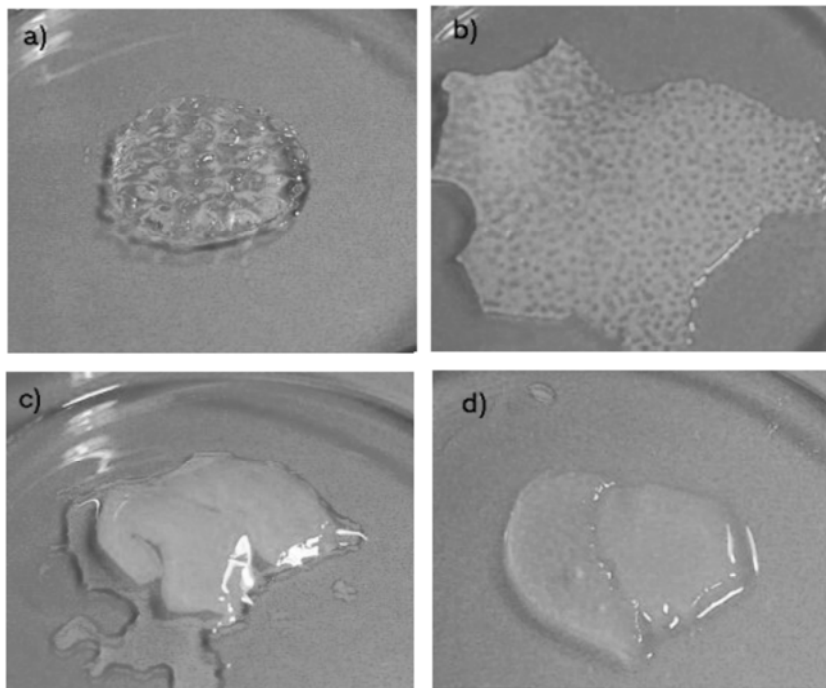
Figure 4.2: PNIPAAm gels prepared by free radical polymerisation using acetone: water and THF: water mixed solvent systems.

Table 4.3: Composition and appearance of gels 1-9 prepared by radical polymerisation.

Gel No.	R	Co-polymerisation medium	Solvent : water Vol%	MBA Mol %	Appearance
1	90	Water	100	1.1	Transparent
2	70	Water	100	1.4	Transparent
3	50	Water	100	2.0	Transparent
4	30	Water	100	3.2	Transparent
5	10	Water	100	9.1	Opaque
6	90	Acetone: water	30:70	1.1	Translucent
7	90	Acetone: water	50:50	1.1	Opaque
8	90	THF: water	30:70	1.1	Translucent
9	90	THF: water	50:50	1.1	Translucent

The phase separation of P(NIPAAm-*co*-MBA) hydrogels co-polymerized in mixed solvents is believed to be due to the co-non-solvency phenomena (Zhang et al., 2008). It is known that some polymers dissolve in pure solvents but are insoluble in their mixtures. PNIPAAm is soluble in water and pure organic solvents such as THF,

acetone, and phenol. However in solvent/water mixtures PNIPAAm solubility is drastically reduced, and the PNIPAAm chains collapse such that two phases form resulting in a heterogeneous structure (Zhang et al., 2008; Zhang et al., 2002b). Zhang *et al* suggested that in a two-phase reaction system, when the polymer chains collapse during polymerization, termination of chain ends are hindered resulting in a higher fraction of dangling chains in the hydrogel, and the effective cross-linking density in the gels are lowered due to the difficulty in cross-linking (Zhang et al., 2002b).

From physical handling, the solvent: water gels were substantially weaker compared to the water series gels. The THF gels showed poorer stability compared to the acetone gels, as they easily broke up even when gently handled. This will represent a significant challenge if for e.g. the hydrogels were to be used for cell culture. Due to the poorer stability of the mixed solvent gels, only DSC and swelling-deswelling studies were conducted using these gels and no other further work was done.

4.3.3 Determination of LCST by DSC

DSC was used to determine the LCST of the P(NIPAAm-*co*-MBA) hydrogels. During heating from 10-60 ℃, all of the hydrogels develop ed an endothermic peak (**Figure 4.3**), which indicates that the hydrogels underwent shrinking upon heating.
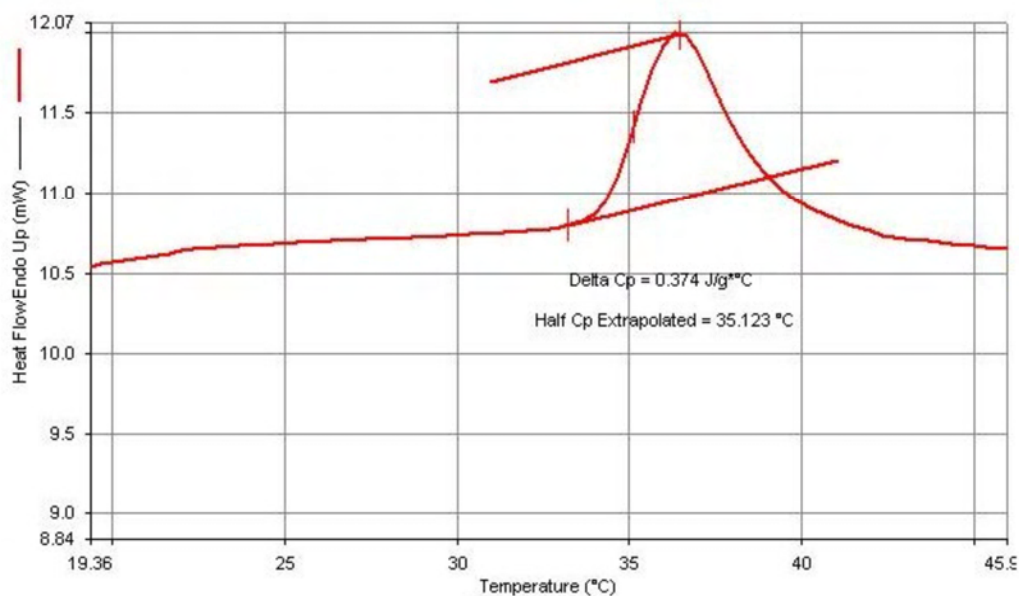

Figure 4.3:   Typical DSC thermogram of P(NIPAAm-co-MBA) hydrogel with R 90 showing the LCST (endotherm is down).

The LCST was taken as the onset to the peak maximum and is the point at which the polymer network collapses and water is released. The average LCST's of the P(NIPAAm-*co*-MBA) hydrogels with varying cross-link densities are tabulated in **Table 4.4**. It was found that for all of the water series hydrogels (R 90-10), the LCST varied between 34-35 ℃ and was independent of the cross-linker range investigated (i.e. 1.1-9.1 Mol% MBA). Our findings has been corroborated with other studies reported in the literature (Zhang et al., 2003). It can be concluded that the overall hydrophilicity/hydrophobicity balance of the P(NIPAAm-*co*-MBA) gels was maintained in this MBA range. Even though MBA contains hydrophilic amide groups which would increase polymer-water interaction, in the cross-link range investigated, it can be assumed that the hydrophilic effect is counterbalanced by the additional methylene groups in MBA, which contribute to higher hydrophobic-hydrophobic interactions, thereby balancing the hydrophilic effect of the amide groups. The LCST of all the P(NIPAAm-*co*-MBA) hydrogels was higher than that of linear PNIPAAm (LCST = 32 ℃) indicating that the presence of MBA increased hydrogen bonding with water due to an increase in amide groups.

Table 4.4:   Average LCST of P(NIPAAm-*co*-MBA) hydrogels determined by DSC with MBA cross-link density from R 90-10 (i.e. 1.1-9.1 Mol% MBA) (n=5).

R	MBA Mol %	LCST /°C	Copolymerisation medium
90	1.1	34 ± 1	Water
70	1.4	35 ± 1	Water
50	2.0	34 ± 0.4	Water
30	3.2	35 ± 0.9	Water
10	9.1	35 ± 0.4	Water
90	1.1	33.8 ± 0.5	30:70 Acetone: water
90	1.1	32.9 ± 0.3	50:50 Acetone: water
90	1.1	33.4 ± 0.4	30:70 THF:water
90	1.1	33.3 ± 0.3	50:50 THF:water

The LCST's of all the mixed solvent gels was lower than the pure water series gels, and on average ranged between 32-33 ℃. Similar res ults have also been reported previously for P(NIPAAm-co-MBA) gels with increasing THF:water content (Zhang et al., 2002b). According to Zhang *et a*l. the reduced LCST's for the mixed solvent gels, indicate that freed water diffuses out of the heterogeneous polymer networks more

easily than for the gels made in water (Zhang et al., 2002b). Hence it is expected that the de-swelling of the gels when prepared in the mixed solvents will be faster than for the homogenous standard gels.

For the PNIPAAm water-series hydrogels with R 90-30, the phase transition could be clearly observed visually by placing the hydrogels in an oven at 37 ℃. Upon heating to 37 ℃, the clear transparent hydrogels turned op aque and formed a white precipitate as shown in **Figure 4.4**. For the R 10 gel however which was already opaque at room temperature following polymerisation, and the change could not be visually detected by the naked eye upon heating at 37 ℃.
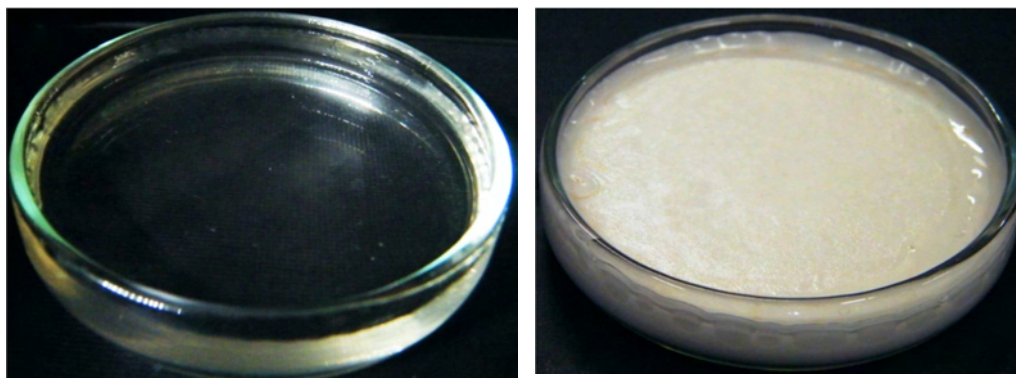

Figure 4.4:   Phase transition of P(NIPAAm-*co*-MBA) hydrogel (R 90 gel) , showing the clear transparent hydrophilic state at 23 ℃ (l eft), and the hydrophobic state when heated to 37 ℃ (right).

4.3.4 Morphology

From literature, the morphology of PNIPAAm hydrogels is investigated using scanning electron microscopy (SEM), whereby the hydrogels are first immersed in liquid nitrogen followed by freeze drying (Caykara et al., 2006a; Zhang et al., 2003). However it is known that the cold treatment of the hydrogels can cause ice crystal artefacts which can increase the porosity of the hydrogels (Zhang et al., 2008). In Zhang *et al.* mention is made of "structural artefacts" due to the SEM preparation procedure, and therefore it was suggested that only structural differences between samples should be considered (Zhang et al., 2004). However this raises some scepticism regarding the "true" morphology of PNIPAAm hydrogels which have been previously reported. In this study the real morphology of the P(NIPAAm-*co*-MBA) hydrogels was investigated using ESEM. ESEM does not require any sample

treatment prior to imaging. The ESEM studies were performed at the Centre for Electron Microscopy at the University of Kwazulu Natal in Pietermaritzburg. The ESEM images of the PNIPAAm hydrogels prepared in water appear in **Figures 4.5-4.6**.
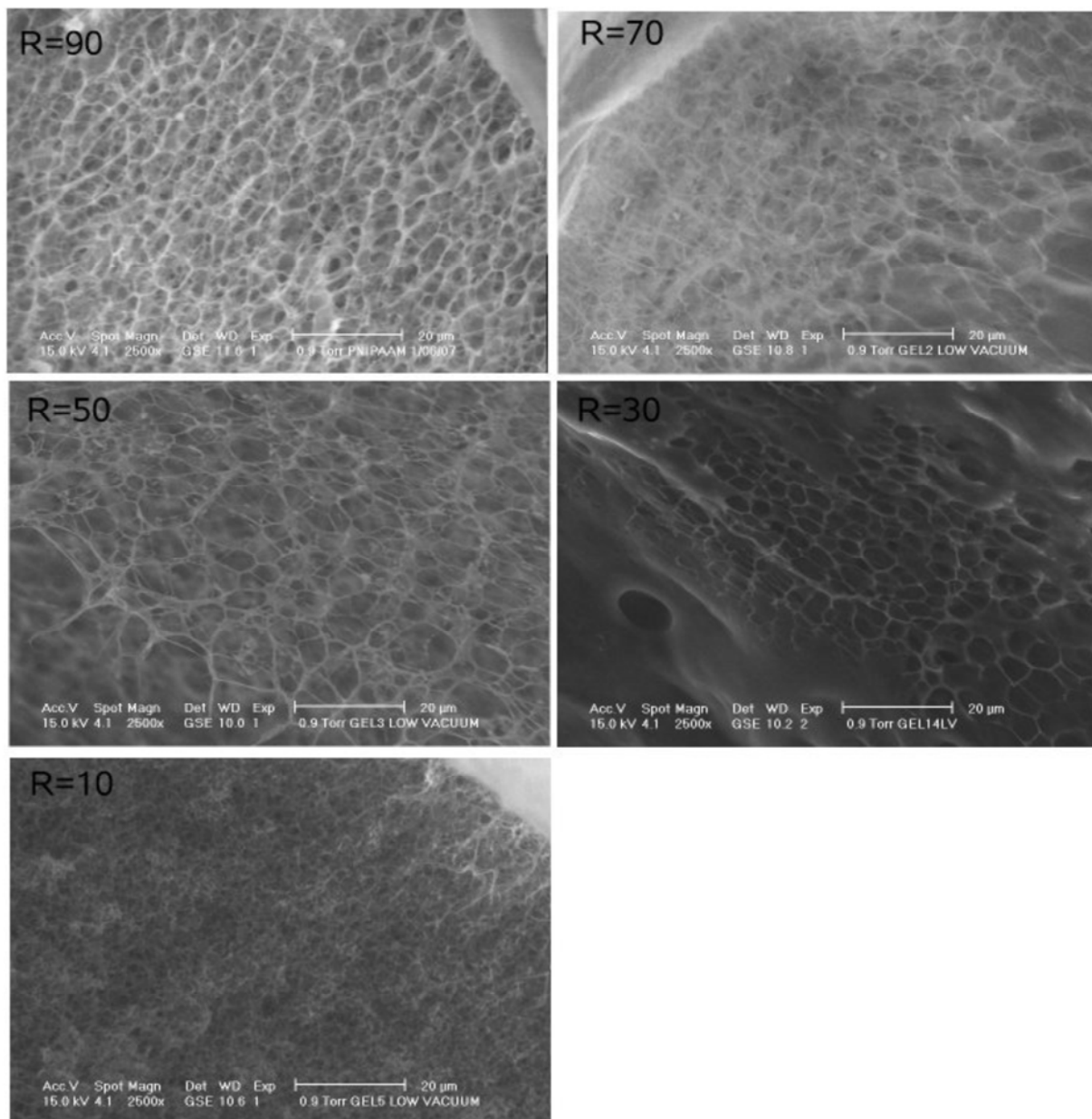

Figure 4.5:   ESEM images of P(NIPAAm-*co*-MBA) hydrogels prepared in water with a cross-link density R ranging from 90 to 10 at 25 °C.
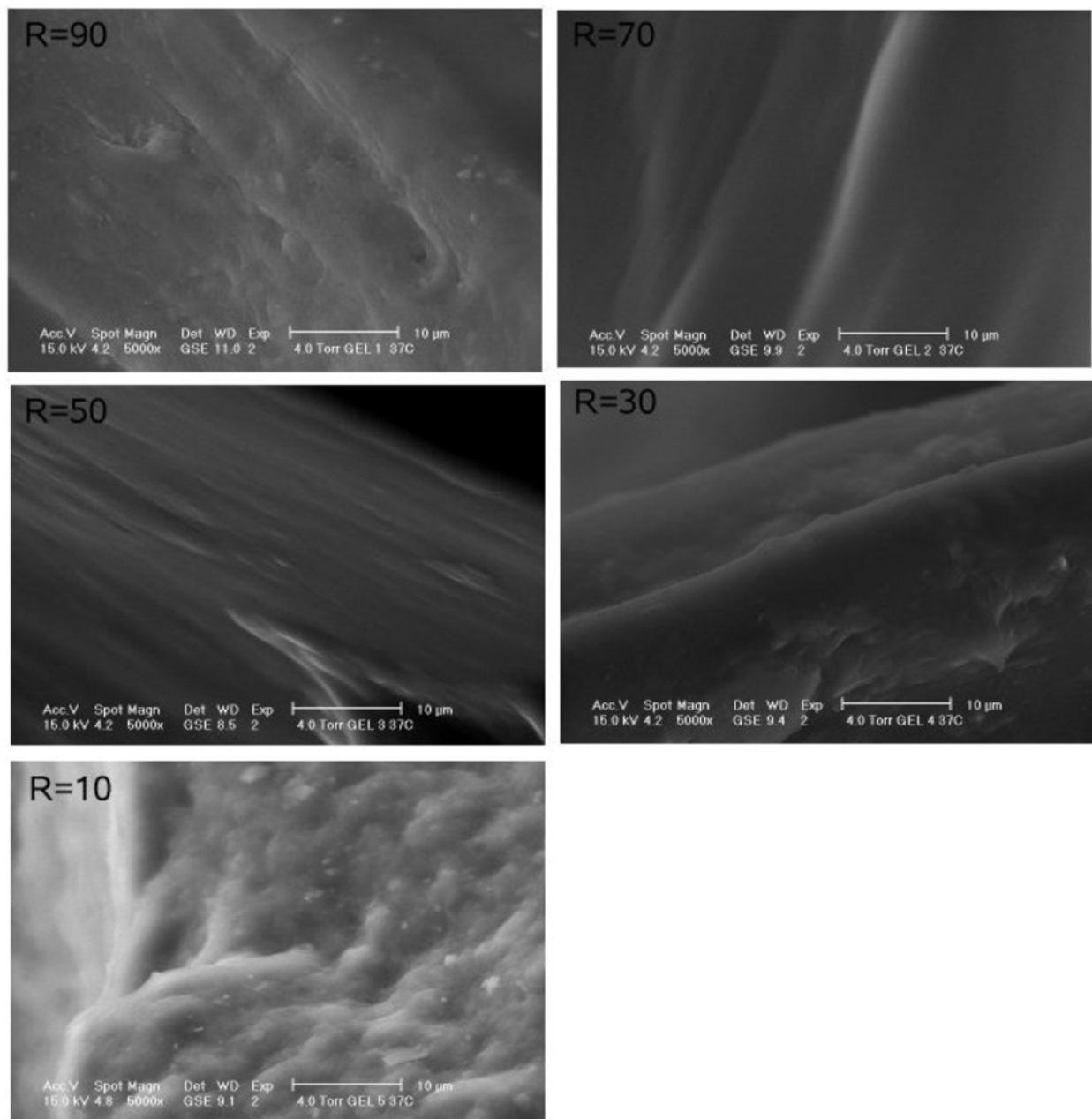
Figure 4.6:   ESEM images of P(NIPAAm-*co*-MBA) hydrogels prepared in water with a cross-link density ranging from 90 to 10 at 37 °C.

From the ESEM images, it could be seen that all of the hydrogels displayed porous structures at 25 °C (**Figure 4.5**), while when equilibrated at 37 °C all of the hydrogels underwent a phase transition, and collapsed into dense structures with complete loss of porosity (**Figure 4.6**). The pore sizes in the R 90 gel (at 25 °C) was less than 10 μm and it can be seen that the pore sizes tended to decrease as the cross-link density was increased. The pores in gel R 10 appeared substantially smaller and more uniform compared to the gels with less cross-linker. For gel R 30 however it seems that part of the surface may have dried out during the imaging at 25 °C (**Figure 4.5**).

103

Zhang *et al.* studied the effect of cross-link density on the morphology of P(NIPAAm-*co*-MBA) hydrogels and they also reported that pore size decreased as the cross-link density was increased (Zhang et al., 2003). It is well known that for hydrogels with an increasing cross-link density, the molecular mass between cross-links are reduced, which results in an increase in pore density in the network structure (Caykara et al., 2006a).

The collapsed dense surface at 37 °C is indicative of the skin layer formation during de-swelling. It has been reported that PNIPAAm hydrogels display a dense skin layer which contributes to the slow de-swelling rate of the gels (Zhang et al, 2008). However it was observed that in the hydrophobic state, porosity is largely lost which implies that if cells were to be attached onto the hydrogels in the hydrophobic state during cell culture, they will be unable to grow in a structural 3D environment. It was reported previously (see Chapter 1) that highly porous scaffolds with interconnected pores in the size range of 100-300 µm are desirable for cell culture, since they enable optimal cell-cell interactions, while allowing for oxygen and nutrient supply to the cells. Additionally in the hydrophilic state, pore sizes are relatively small (<10 µm), and if cells penetrate into the hydrogel, cell release might be a challenge due to the path tortuosity in the hydrogels, whereby cells may become entrapped in the matrix. The use of mixed solvent systems during co-polymerisation may improve the porosity of the hydrogels; however this aspect was not investigated due to the relatively poor stability of the hydrogels. Zhang et al., 2002a prepared cross-linked PNIPAAm hydrogels in THF: water, and observed that in the shrunken state, some porosity was retained in the gel structure. However when dehydrated the pores were in the sub-micron range, which is undesirable for cell culture.

4.3.5 Swelling and de-swelling properties

1) Swelling Ratios

The maximum swelling ratios of the P(NIPAAm-*co*-MBA) hydrogels appear in **Table 4.5**. Firstly it was observed that when mixed solvents were used as the co-polymerisation medium (gels 6-9), the equilibrium swelling ratios were far superior compared to when water was used (gels 1-5). The 50:50 THF: water gels displayed the highest swelling ratio of ~48.3 ± 1.5 (i.e. ~ 4800% increase in weight). The equilibrium swelling ratios were found to decrease in the following order:

50:50 THF:water > 30:70 THF:water > 50:50 acetone:water > 30:70 acetone:water >100% water.

Table 4.5:   The average equilibrium swelling ratios of PNIPAAm hydrogel prepared in water (R 90-10); acetone : water (R 90) and THF:water mixtures (R90). N=5.

Gel No.	R	Co-polymerisation medium	Swelling ratio
1	90	Water	16 ± 0.3
2	70	Water	16 ± 0.4
3	50	Water	12 ± 0.08
4	30	Water	11 ± 0.1
5	10	Water	11 ± 0.3
6	90	Acetone: water	21.7 ± 4.3
7	90	Acetone: water	33.6 ± 2.1
8	90	THF: water	45.3 ± 4.2
9	90	THF: water	48.3 ± 1.5

It was also observed that the maximum swelling ratios of the hydrogels was dependent on the cross-link density, such that with increasing MBA content, the equilibrium swelling ratio of the hydrogels decreased. It is believed that as the cross-link density increases, the expansion of the network structure and the free volume within the hydrogel network is reduced hence the swelling capacity of the hydrogels is also reduced (Caykara et al., 2006a; Zhang et al., 2003). For the water series gels, when R was 90 (i.e. the lowest cross-linker content), swelling ratio reached a maximum of $\sim 16 \pm 0.3$ (n=5). This is in accordance with that observed by Zhang et al [2002] for PNIPAAm hydrogels. They have shown that the diffusion coefficient in PNIPAAm hydrogels decreases with an increase in MBA concentration. Additionally the reduced swelling of highly cross-linked networks has also been attributed to the glassy inner core of dried hydrogels (Caykara et al., 2006a; Zhang et al., 2003). Prior to swelling, in the dry hydrogel, there are strong intermolecular or polymer–polymer interactions, such as hydrogen bonds and hydrophobic interactions, which remain in a glassy state (Caykara et al., 2006a; Zhang et al., 2003). It has been suggested that in hydrogels with higher cross-linking, these interchain interactions are enhanced which leads to a significant reduction in water uptake (Caykara et al., 2006a).

The high swelling ratios of PNIPAAm gels polymerised in mixed solvents indicate highly porous and interconnected structures for the hydrogel networks. According to Zhang *et al*, polymer chains are widely expanded in the mixed solvents during polymerisation, and upon swelling in pure water, the solvent in the gel network is replaced by water, but the gel keeps its widely expanded state, which leads to large equilibrium swelling ratio of the gels (Zhang et al., 2002a). The mixed solvent gel series can be classified as "superabsorbent hydrogels" which are defined as hydrogels which absorb more than 20 times their own weight while maintaining their shape (Geever et al., 2007). Similar ratios have been reported previously for THF:water gels at 25 ℃ (Zhang et al., 2002b), howe ver for PNIPAAm gels prepared in 50:50 and 30:70 acetone:water mixtures previous studies report higher swelling ratios in the range of 45-55 (Zhang et al., 2002a). Although the formulations were similar to that reported in this study, discrepancies may be due to uncontrolled solvent evaporation in the present study.

2) *Swelling kinetics*

The swelling kinetics for the P(NIPAAm-*co*-MBA) hydrogels at 20 ℃ prepared in solvent : water mixtures are shown in **Figure 4.7**.
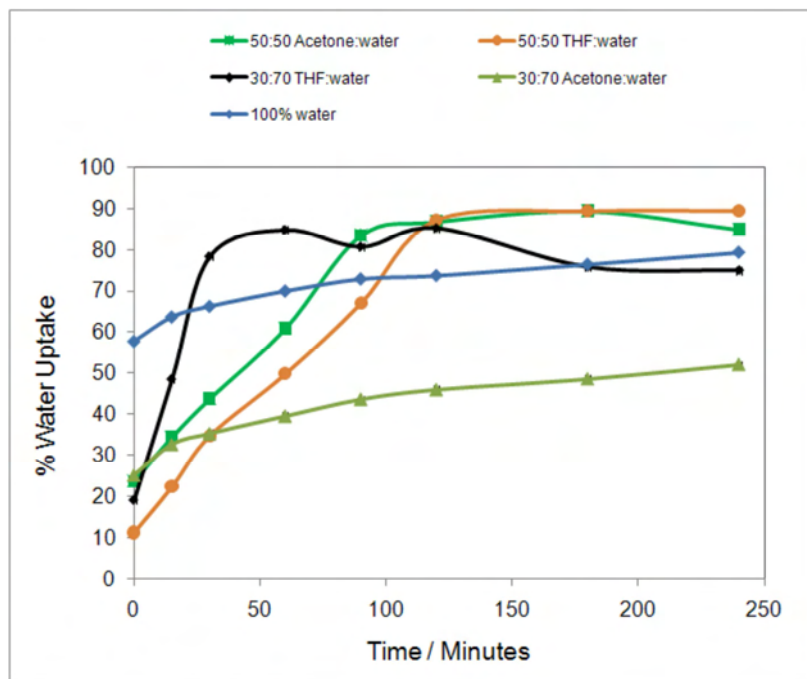

Figure 4.7:   Swelling kinetics at 20 ℃ showing the percent wa ter uptake of partly swollen P(NIPAAm-*co*-MBA) hydrogels which were prepared in solvent : water mixtures with R 90, after air-drying for 24 hours. (Average taken of five samples.)

Prior to the kinetic studies, the polymerised gels were left open to air-dry for 24 hours. Since the gels were not completely dried it can be seen that at the start of the kinetics, gels were already partly swollen. Due to the higher solvent content in the solvent:water series gels these gels displayed higher solvent evaporation and hence lower initial swelling was observed at time zero compared to the 100% water gel. The 30:70 THF:water gel showed the fastest response rate and in just 15 minutes the percent water uptake increased from $19 \pm 2\%$ to $49 \pm 10\%$. After an hour, the water uptake reached $85 \pm 11\%$.Comparisons cannot be made to the standard PNIPAAm gels without solvent due to its higher initial water content. At 90 minutes both the 50:50 acetone:water and 50:50 THF:water reached ~80% water uptake. The 30:70 acetone:water gels however deviated from this trend and showed a very slow response whereby water uptake increased from 25 ± 9 at the start of the study to 52 ± 14 in 240 minutes. Large deviations were observed for the swelling ratios for all of the solvent series gels, which may be due to uncontrolled solvent evaporation during polymerisation.

It is known that swelling of hydrogel networks is a diffusion-controlled process which is thermodynamically driven. For the 30:70 THF:water; 50:50 THF:water and 50:50 acetone:water gels, swelling proceeded in two stages i.e. the initial stage was very rapid as water easily penetrated into the polymer network, and as the sample approached complete hydration in the second stage of swelling, the rate of water diffusion levelled off. This is believed to be due to the retractive force due to the cross-linking in the hydrogel structure which counterbalances the thermodynamically driven swelling process (Geever et al., 2007). The swelling kinetics of the R series gels prepared in water is given in **Figure 4.8**.

Since water was used as the co-polymerisation medium, all the gels were already highly swollen at the start of the swelling kinetics which has influenced the swelling rate reported here. Swelling kinetics was found to be dependent on the cross-link density. PNIPAAm hydrogels with the lowest cross-link densities i.e. R 90- 50 showed the fastest water uptake, while gels R 30 and 10 were the slowest. Since the gels of the present study were left to equilibrate for 24 hours prior to the kinetic studies, and already contained about 50% of its total water content, it can be assumed that the trend depicted in **Figure 4.8**, is probably for the second stage of swelling where rapid diffusion is no longer possible.
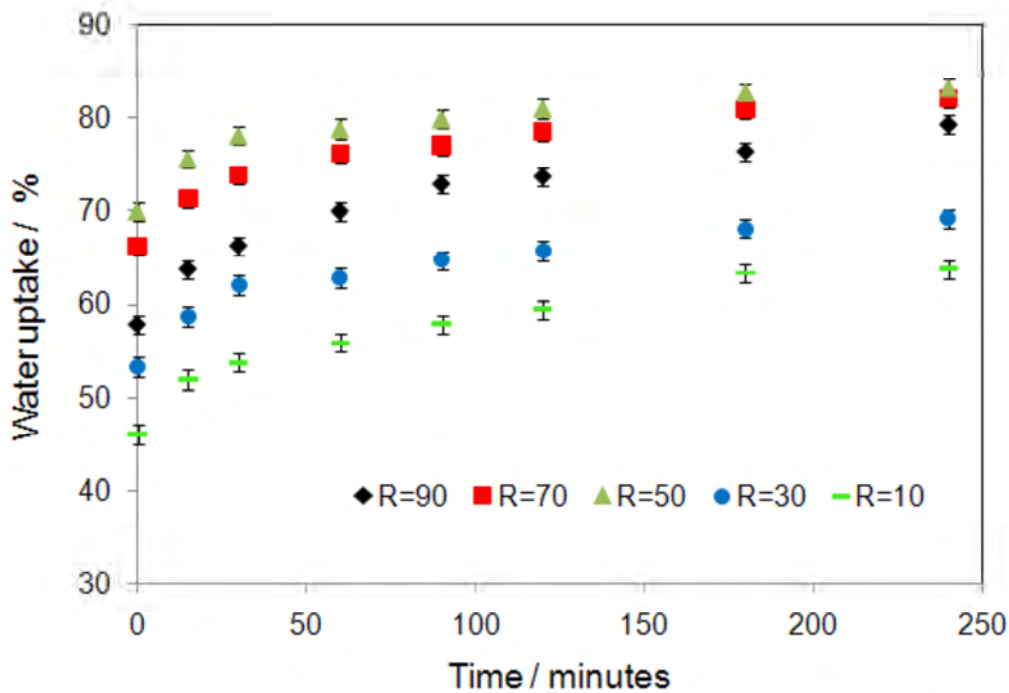
Figure 4.8: Swelling kinetics at 20 °C showing the percent wat er uptake of partly swollen P(NIPAAm-*co*-MBA) hydrogels which were prepared in water with varying cross-link densities, after air-drying for 24 hours.

Zhang *et al* prepared PNIPAAm hydrogels with a similar cross-link density to the present study (Zhang et al., 2003). They also showed an increase in swelling ratio of the PNIPAAm hydrogels with a decrease in cross-link content, however for water uptake, they reported the opposite trend, i.e. water uptake increased for gels with a higher cross-link density. Swelling of hydrogels is a complex process and is dependent on a number of network parameters as well as the pre-treatment prior to swelling. In the former study, hydrogels were completely dried either directly in a vacuum, or they were heated to 50 °C and then place d in a vacuum oven at 60 °C. It is known that the pre-treatment of the hydrogels plays a major role in the swelling kinetics (Zhang et al., 2003).

3) *De-swelling*

De-swelling kinetics at 37 °C for the solvent:water PNIPAAm hydrogels appear in **Figure 4.9.** As can be seen the response rate for the mixed solvent gels was very rapid when compared to the standard gel which was prepared in pure water. Again the 50:50 THF:water gels showed the fastest response rate whereby in just 10 minutes the percent water retention decreased from 100% to $12 \pm 1\%$, as compared

to 90 ± 0.6% for the standard gel at the same time period. The results indicate that the solvent : water PNIPAAm may be better suited for use in cell culture in terms of deswelling rates compared to the pure water gels.
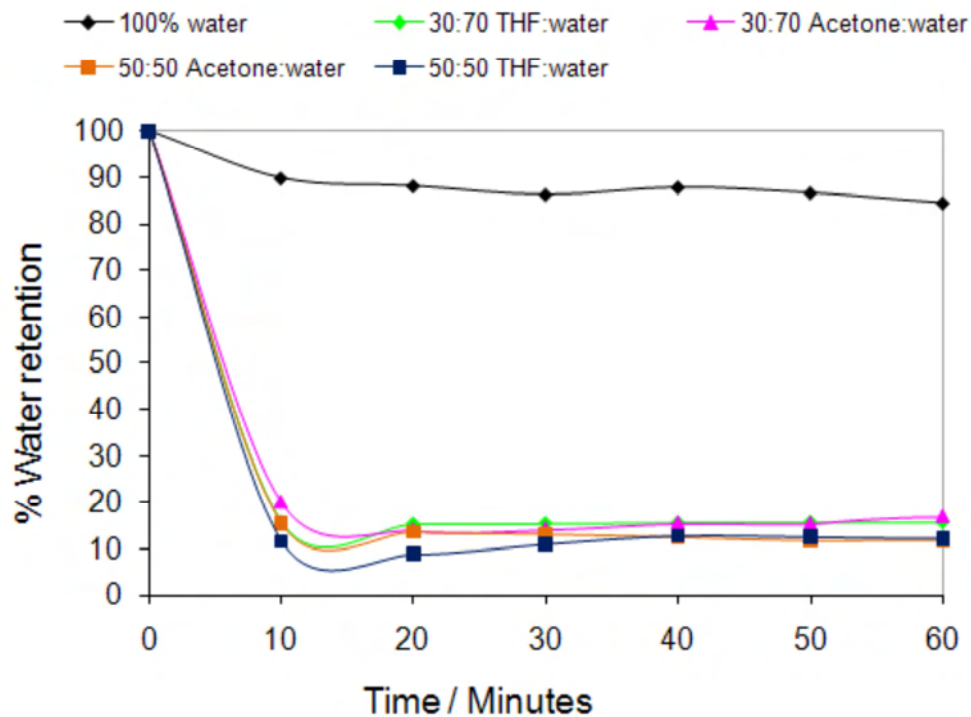

Figure 4.9:   Percent water retention at 37 ℃ for P(NIPAAm- *co*-MBA) hydrogels synthesised in acetone:water and THF:water series. (Average taken of five samples.)

For most of the hydrogels, de-swelling proceeded in two steps, i.e. the initial phase was rapid and thereafter de-swelling slowed down. It is believed that the initial rapid phase is due to rapid diffusion of water out of the hydrogel network, while during the second phase the collapsed skin layer at the outermost surface of the hydrogels prevents the outward flow of water loss and de-swelling then is significantly reduced (Zhang et al., 2003).

It should be noted that de-swelling was performed at 37 ℃ which is very close to the LCST of the P(NIPAAm-*co*-MBA) hydrogels which in this case was found to be between 33-35 ℃ hence a very rapid de-swelling rat e was not seen. To enhance de-swelling, other groups have conducting de-swelling kinetics studies at much higher temperatures, e.g. 50 ℃ (Zhang et al., 2003).

The de-swelling kinetics in this study was performed at 37 ℃ (i.e. body temperature) since is the practical temperature for a number of applications, such as cell culture, drug delivery etc. Zhang *et al* suggests that the very rapid de-swelling of mixed solvent gels can be attributed to the existence of a non-equilibrated shrinking force in the heterogeneous networks, at different collapsed regions, whereby water rich and precipitated polymer rich phases exist in the hydrogel, and during shrinking the water release regions connect with each other forming interconnected water release channels resulting in quick water release from the heterogeneous hydrogel (Zhang et al., 2008). It has also been suggested that the interconnected porous structures of gels prepared in mixed solvents is responsible for the formation of a less dense surface skin layer during shrinking compared to the bulk PNIPAAm gels prepared in water (Zhang et al., 2002b). De-swelling kinetics for the water series gels for varying cross-link density appear in **Figure 4.10**.
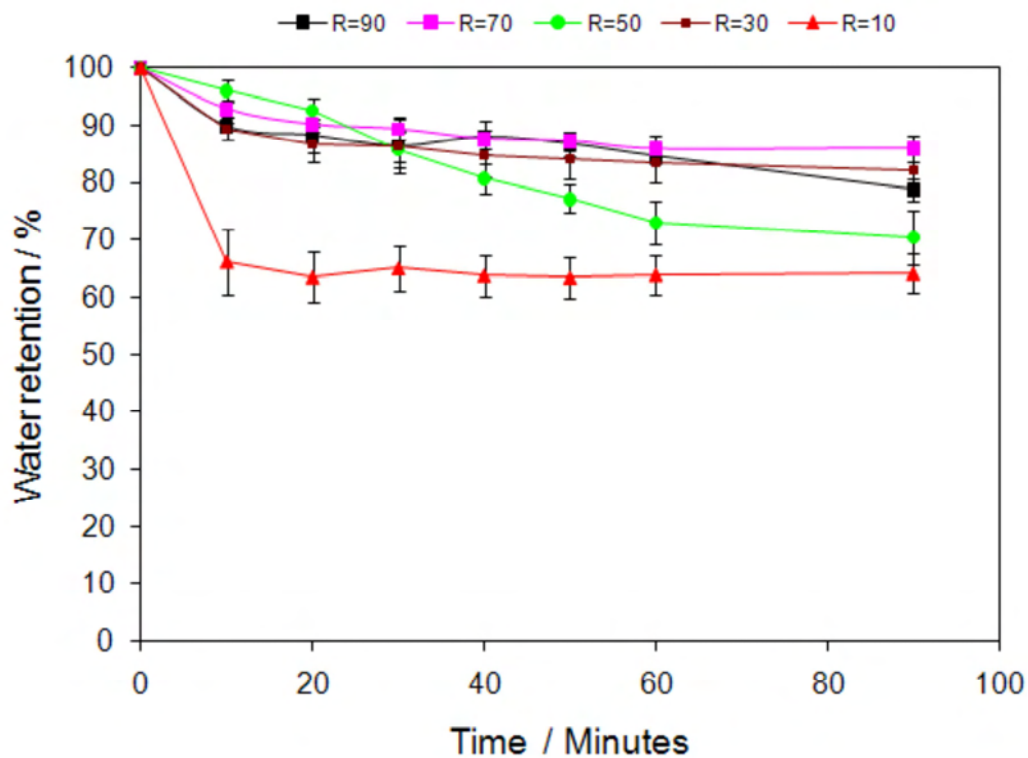

Figure 4.10:   De-swelling kinetics at 37 ℃ for P(NIPAAm-*co*-MBA) hydrogels with varying cross-link density.(Average taken of five samples.)

The de-swelling rates for gels R 90-30 were similar (except for gel R 50 which showed anomalous behaviour). This may be attributed to a similar structure for gels R 90-30. Surprisingly gel R 10 showed the fastest de-swelling rate, and in 10 minutes

the water retention in the gels were reduced from 100% to 66% $\pm$ 6, whereas the water retention in the other gels were around 90% and higher for the same time period. This behaviour was unexpected and was initially thought to be anomalous. However according to Zhang *et al*, when the cross-link density of PNIPAAm hydrogels are increased, the skin layer formation is reduced thereby enabling faster de-swelling for hydrogels with higher cross-link density (Zhang et al., 2003). The higher de-swelling kinetics of the R 10 gels then can possibly be attributed to the formation of a more permeable skin layer and the higher pore density compared to the less cross-linked hydrogels, which creates interconnected water channel which enhance the water diffusion out of the gels. Further repeats are required to confirm the behaviour of the R 10 gel.

4.3.6 Viscoelastic properties

The viscoelastic behaviour of the P(NIPAAm-*co*-MBA) gels (prepared in water) was determined using dynamic shear rheology. The storage (elastic) G′ and loss (viscous) modulus G″ of the gels as a function of strain appear in **Figure 4.11.** The storage modulus refers to the elastic component of a hydrogel, and is an indication of the elastic strength or stiffness of the polymer network. The loss modulus refers to the viscous component of the complex modulus. For all the gels, the storage modulus remained constant with an increase in strain up until the linear viscoelastic (LVE) region, beyond which a sudden drop in storage modulus was observed for each gel. It can be assumed that beyond the LVE region, the gels become mechanically unstable which results in a decrease in the elastic strength of the gels. In contrast, the loss moduli continuously increased with increasing deformation. An increase in G″ suggests that as the strain increases, molecular interactions in the flexible networks of the hydrogels are increased (DeRossi et al, 1991).

Both storage and loss modulus was found to be dependent on the cross-link density. With an increase in cross-link density (i.e. decreasing R), storage and loss moduli, as well as tan δ increased (**Figure 4.12**). It was observed for all of the hydrogels, that G′ > G″ by more than an order of magnitude, which indicates a viscoelastic gel (Garbern et al., 2010). Additionally tan δ was <1 for the whole cross-link range confirming a gel structure (Garbern et al., 2010).
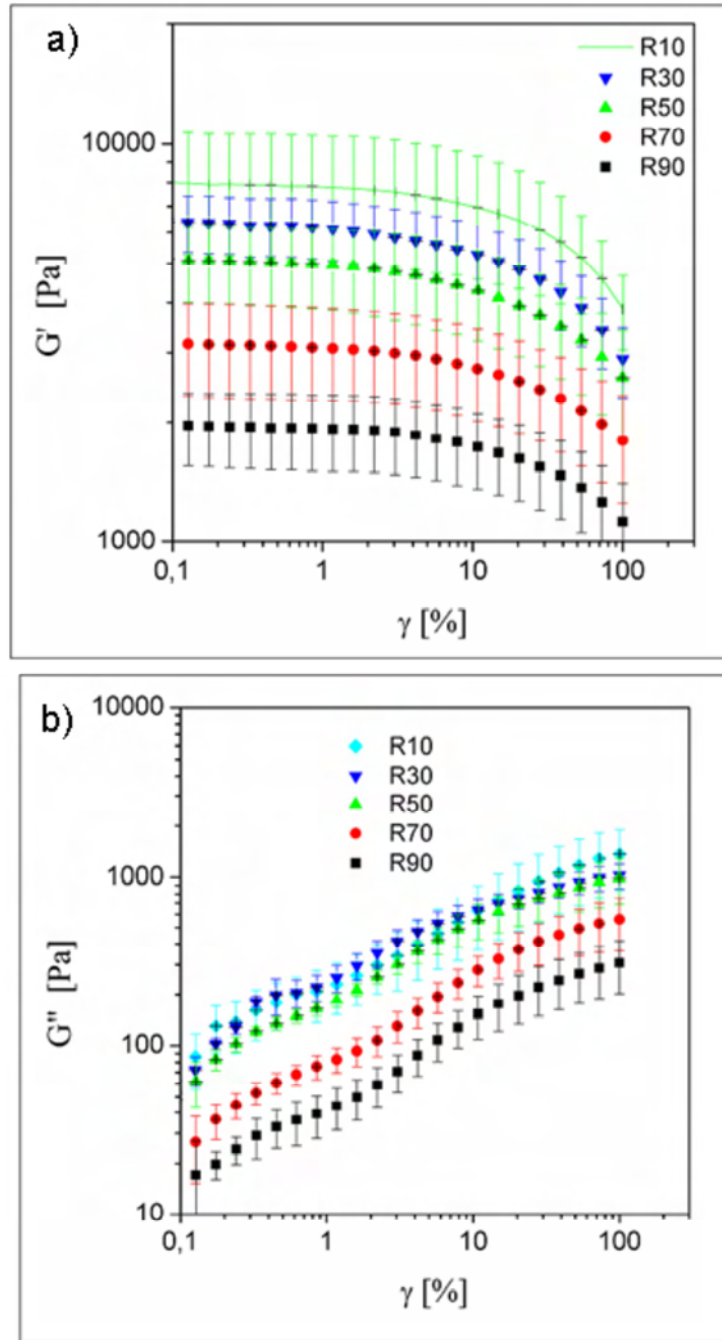
Figure 4.11: Storage modulus (G′) (a) and loss modulus (G″) (b) as a function of strain (γ) for P(NIPAAm-*co*-MBA) hydrogels with cross-link density R 90-10 at 25 °C (with ω =10 s⁻¹).

It appeared that tan δ displays a maximum at R 30. However on further analysis (from temperature and frequency sweeps), it was realised that gel R 10 behaved anomously due to gel heterogeniy. The threshold limit of linear viscoelasticity and the average storage modulus for the R 90-R 10 hydrogels appear in **Table 4.6**. The

strain at LVE and increased with an increasing cross-linker content. For gel R10 the storage modulus at the LVE region was 7143 ± 2467 Pa which was the highest for the gels investigated. This is due to greater elastic strength of the P(NIPAAm-*co*-MBA) gels as the cross-links are increased.
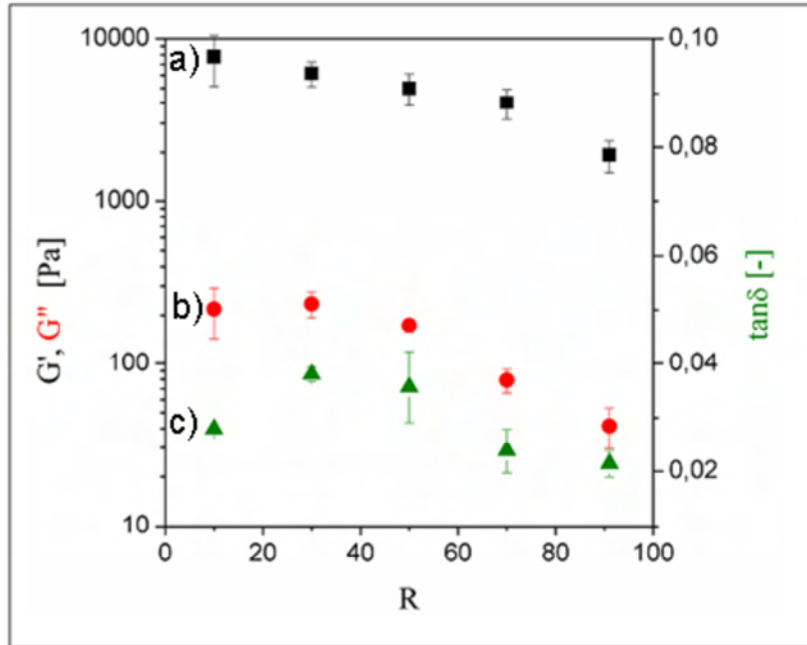

Figure 4.12: The change of a) storage modulus (G′), b) loss modulus (G″) and c) damping factor (tan δ) with decreasing cross-linker content (increasing R) at 25 ℃ with $\gamma = 1\%$; $\omega = 10$ s^{-1}.

Table 4.6: Threshold limit of linear viscoelastic range of P(NIPAAm-*co*-MBA) hydrogels with different cross-link density (γ is the strain, and G′ is the storage modulus).

Gel /R	γ at LVE /%	G′ /Pa	Std dev
90	1.61	1917	417
70	1.89	3036	777
50	2.21	4863	1160
30	5.73	5570	1022
10	7.85	7143	2467

The temperature sweeps to investigate the thermal phase changes of the various hydrogels appear in **Figure 4.13**. Both storage and loss modulus (and hence tan δ) were highly dependent on temperature. As expected, below the temperature of volume phase transition the values of storage, and loss moduli are successively

higher for the gels with higher cross-linker content. Up to the temperature of volume phase transition the moduli decreases with increasing temperature for all the gels.
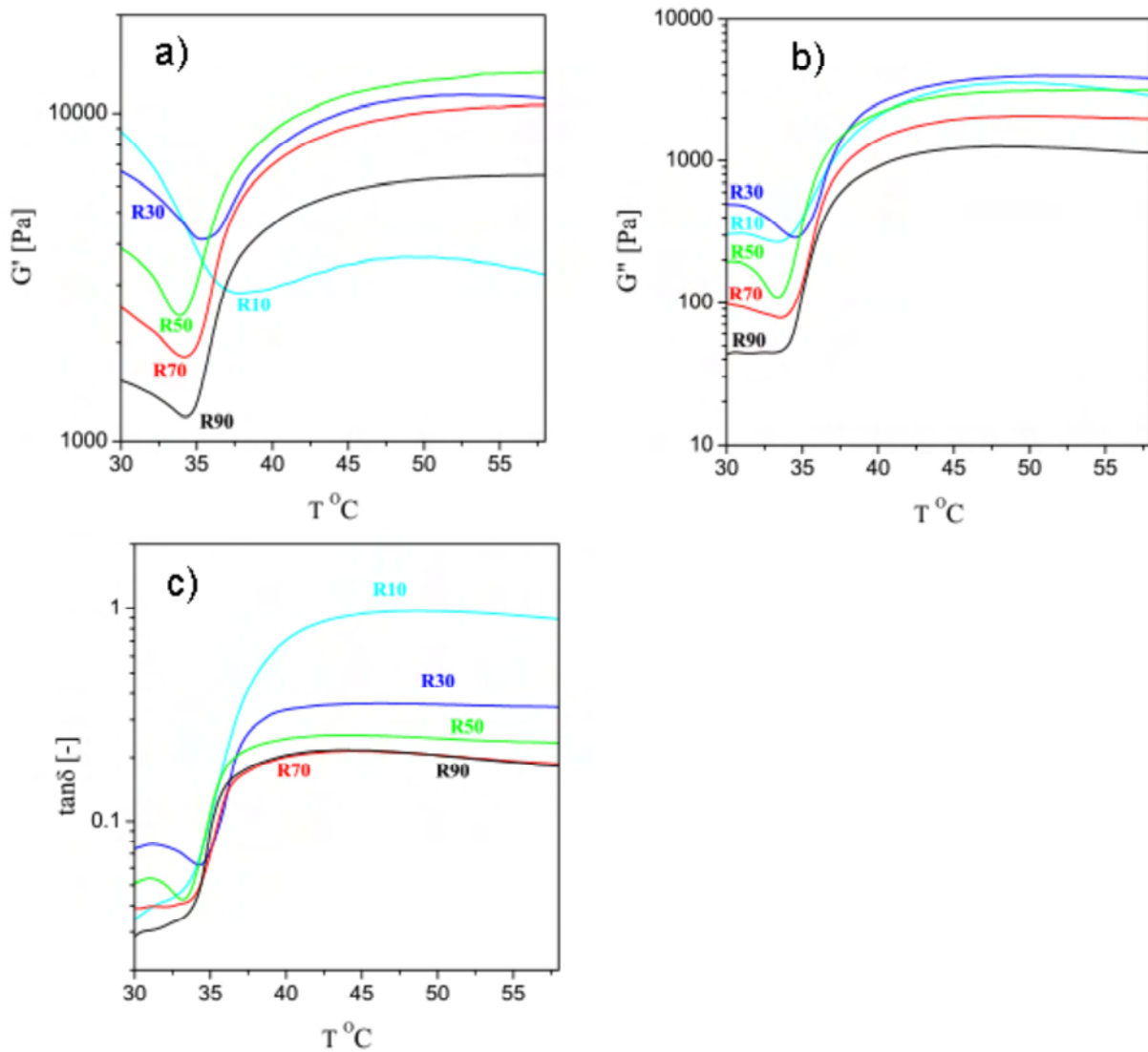

Figure 4.13: (a) Storage modulus (G′); (b) loss modulus (G″) and (c) tan δ as a function of temperature for P(NIPAAm-*co*-MBA) hydrogels R 10-90.

However at temperatures higher than the LCST dramatic increases in both storage and loss moduli were observed for all of the gels (except R 10) until equilibrium is reached. The initial decrease in moduli prior to the LCST was more prominent for G′ than G″. This may be related to a decrease in hydrogen bonding as the temperature approaches the LCST which has a larger impact on the storage modulus. Hydrogen bonds in the hydrogel structure start to break at temperatures close to the volumetric phase transition, as the molecules start to undergo a conformational change from hydrophilic to hydrophobic. At the LCST, both the storage and loss moduli are at a

minimum due to a maximum decrease in hydrogen bonding in the hydrogel structure. However when the temperature is increased beyond the LCST, the G′ and G″ increase which is related to the formation of molecular interaction in the gel at higher temperatures (DeRossi et al., 1991). At the LCST the polymer chains undergo coil to globule conformation which may result in enhanced aggregation resulting in an increase in loss modulus (Lessard et al., 2003). Additionally hydrophobic interactions between the polymer chains are favoured above the LCST which result in greater elastic strength (storage modulus) of the hydrogels. The behaviour of gel R 10 was found to be anomalous, and was attributed to heterogeneous cross-linking during polymerisation due to the higher cross-linker content.

The LCST of the P(NIPAAm-*co*-MBA) hydrogels was also determined from the storage modulus, loss modulus, and tan δ and the LCST values appear in **Table 4.7**. The LCST of all the hydrogels ranged between 32-34 °C which was slightly lower than that measured by DSC. Also the cross-link density in the investigated range of MBA concentration (1.1-9.1 Mol% MBA) did not affect the temperature of volume phase transition which corroborates with the DSC data. Although when 9.1 Mol% MBA was used, this resulted in a broader temperature range of transition of Gel R 10 which may be due to the heterogeneity of the polymer system (**Figure 4.13c**).

Table 4.7:   Onset temperature of volumetric phase transition for hydrogels with different cross-link density from dynamic rheometry.

R	LCST from G′ /℃	LCST from G″/℃	LCST from Tan δ /℃
90	33.8 ± 0.5	33.3 ± 0.6	33.0 ± 0.1
70	33.8 ± 0.2	33.3 ± 0.2	33.2 ± 0.1
50	33.2 ± 0.3	33.0 ± 0.2	33.0 ± 0.1
30	34.4 ± 0.2	33.2 ± 0.2	33.3 ± 0.2
10	33.1 ± 0.7	32.3 ± 0.1	32.5 ± 0.5

To verify the stability of the P(NIPAAm-*co*-MBA) hydrogels below and above the phase transition temperature oscillatory measurements were carried out with increasing frequency (strain frequency sweep). The change of complex viscosity (η*), storage modulus and loss modulus with angular frequency (ω) below and above the volumetric phase transition for the different gels is given in **Figure 4.14**.
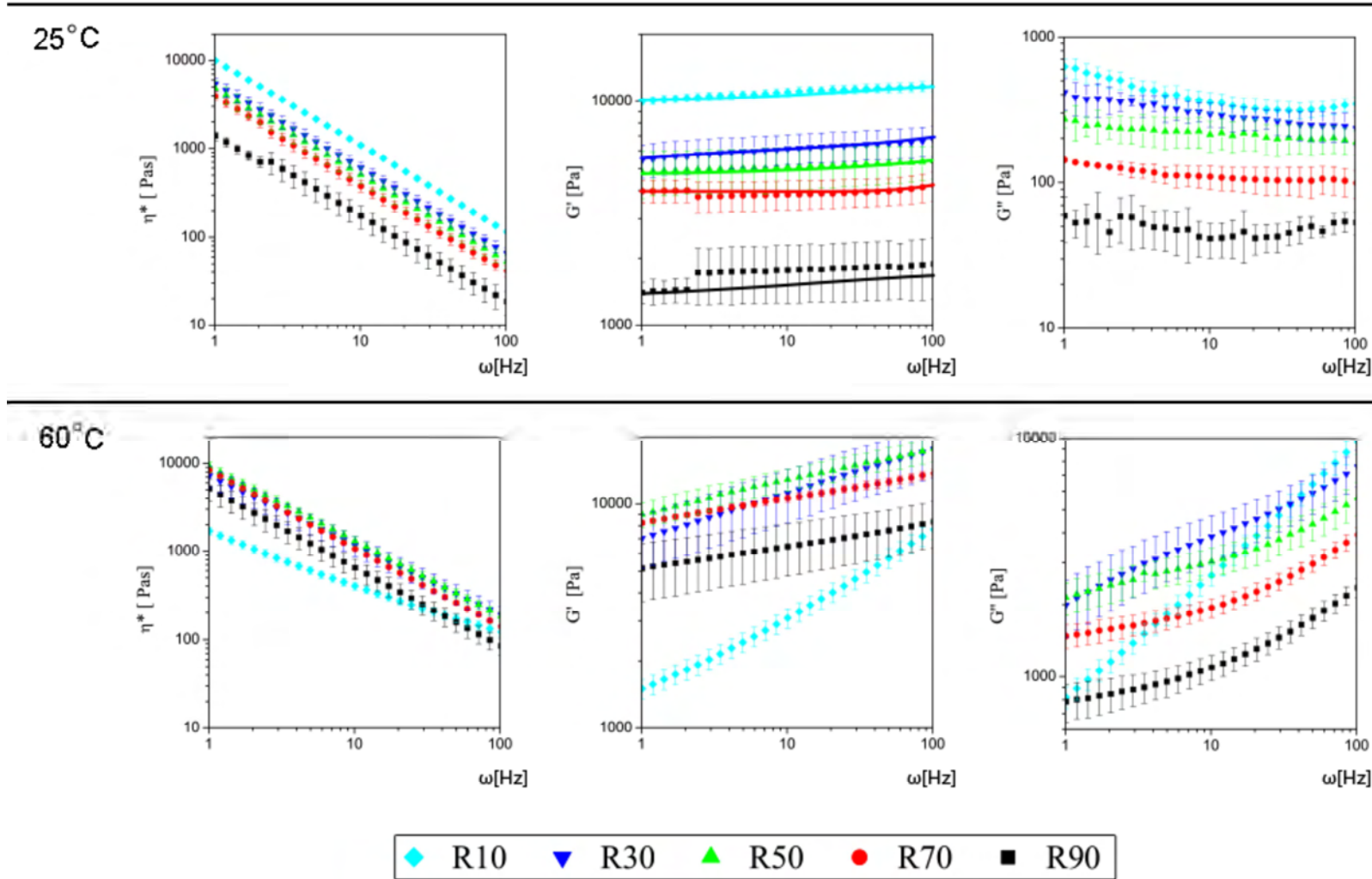
Figure 4.14:   The change of complex viscosity (η^*), storage modulus (G′) and loss modulus (G″) at 25 ℃ and 60 ℃ for the gels with different cross-linker content (γ=1%).

Firstly it was observed that G′ and G″ was independent of the frequency at 25 ℃ and the contribution of the storage (elastic) modulus was the greatest at all frequencies. This behaviour is typical of gel systems (Lessard et al., 2003). However the complex viscosity decreased with an increase in frequency which shows shear thinning which is typical of a polymer solution in water (Lessard et al., 2003). This may indicate that at higher frequencies, the shearing forces disrupt the molecular interaction between the polymer chains in the hydrogel resulting in a decrease in viscosity. This may indicate poor stability of the hydrogel structures. The complex viscosity, storage modulus and loss modulus increased with increasing cross-linker content. Above the phase transition temperature, gel R 10 (at 60 ℃) behaves anomalously just as in case of the temperature sweep. This may be attributed to the heterogeneous polymer structure due to the increased cross-linker. Above the phase transition temperature the hydrophobic gels behave like polymers, meaning that the modulus slightly increases with increasing frequency for each gel, except for gel R 10, where a steep increase in storage modulus was observed.

 A comparison for the storage, loss modulus and tan δ as a function of cross-link density at a frequency of 10 s^{-1} is given in **Figure 4.15**. Below the volumetric phase transition (at 20 ℃) the G′ moduli are about two orders of magnitude higher than the G″ moduli, however above the phase transition (at 60 ℃) substantially highe r loss moduli were observed for the entire cross-link range. This implies that after the phase transition the loss modulus is impacted to a greater extent than the storage modulus. The increase in the loss modulus is indicative of the coil to globule transition at temperatures > LCST which results in precipitation causing increased molecular interaction in the flexible networks (DeRossi, et al. 1991, Lessard et al., 2003).

The viscoelastic properties of the P(NIPAAm-*co*-MBA) hydrogels prepared in mixed solvents were not assessed, since these hydrogels were substantially weaker compared to the R 90 - 10 water series gels. Further work can involve investigating the effect of increasing cross-link density on the mechanical properties of the mixed solvent gels.

4.3.7 Water contact angle

The static contact angle of P(NIPAAm-co-MBA) hydrogels with varying cross-link density at 40 ℃ and at 20 ℃ is given in   **Table 4.8**. Contact angle measurements provide information about the outermost surface layer of the hydrogels. For all of the hydrogels, at 40 ℃ the contact angle values were relatively higher hence the surface was more hydrophobic

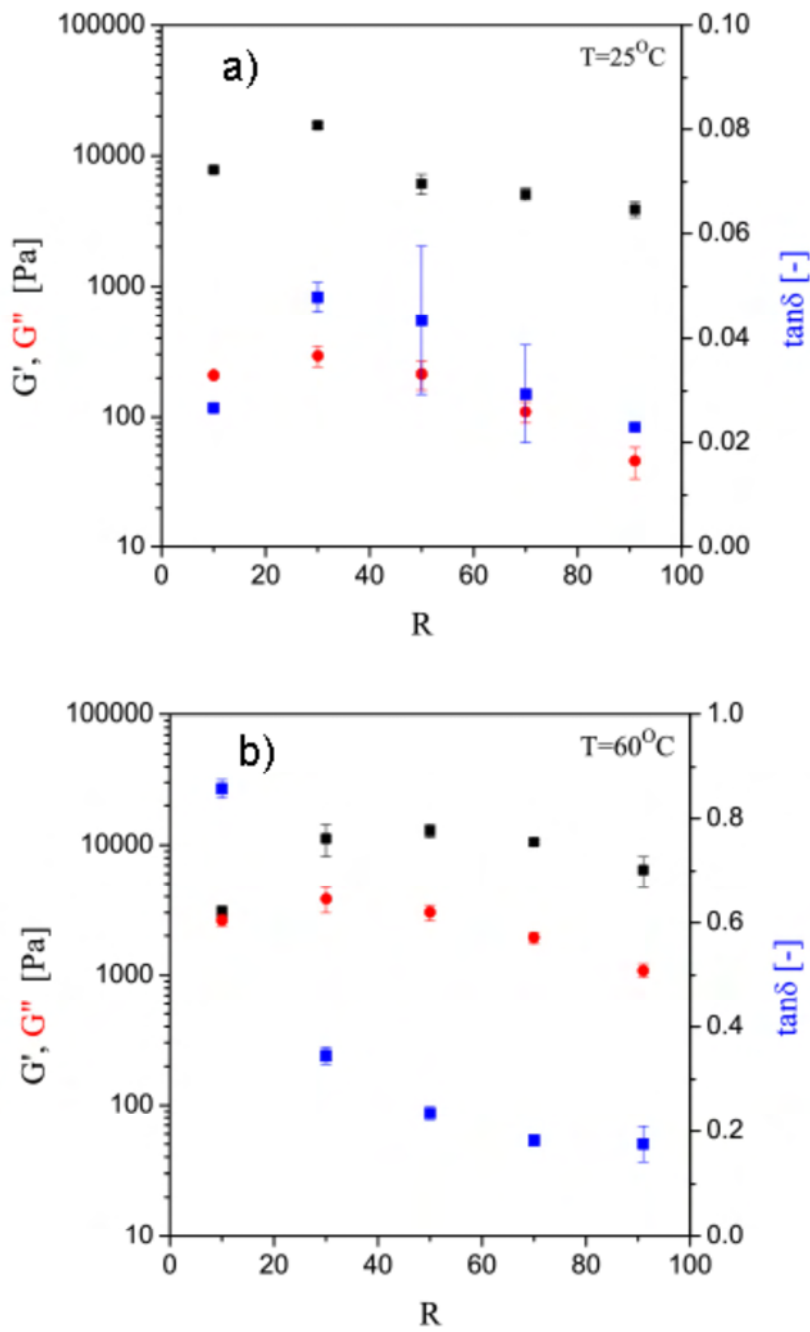compared to 20 ℃ confirming the phase transition o f the surface layers of the PNIPAAm hydrogels.

Figure 4.15: Change in storage modulus, loss modulus and damping factor (tan δ) with decreasing cross-linker content at (a) 25 ℃ and (b) 60 ℃ from frequency sweep measurements at 10 s^{-1} (γ = 1%).

Table 4.8: Static contact angle of P(NIPAAm-*co*-MBA) hydrogels (prepared in water) with varying cross-link density at 40 ℃ and 20 ℃ (n=5).

R	MBA wt%	Contact Angle	
		40 °C	20 °C
90	1.5	86 ± 5	62 ± 5
70	1.9	77 ± 4	57 ± 3
50	2.7	65 ± 4	48 ± 3
30	4.3	62 ± 1	48 ± 5
10	12.0	35 ± 6	23 ± 6

The contact angle was dependent on the cross-link density of the gels. As the cross-link density increased i.e. R decreased, the contact angle values decreased. Even though the surface of the P(NIPAAm-*co*-MBA) gels was relatively more hydrophobic at 40 °C compared to 20 °C, the contact angles were still low, and more so for the higher crosslink gels. This implies that the hydrogels are still hydrated in the hydrophobic state, which may be due to the dense skin layer formation, which retards water expulsion. Gels were equilibrated for 30 minutes prior to contact angle analysis, which is insufficient to dehydrate the gels. These results however do not correlate with the de-swelling studies for the water series gels (R 90 - 10) where we observed the R 10 hydrogel to demonstrate the fastest deswelling for the R series gels.

The change in contact angle with temperature and the effect of cross-link density on contact angle can both be explained by the concept of surface configuration change and surface-state equilibration which occurs on polymer surfaces (Yasuda and Okuno, 1994).

In general polymers, due to their long molecular chains, have the capability to reorient their functional groups at the surface by means of rotational and migrational rearrangement in order to minimise the interfacial tension at the polymer-air interface (Yasuda and Okano, 1994). A high degree of segmental mobility is possible in highly swollen hydrogels. For hydrogels with less cross-linker, greater chain mobility is possible at the gel-air interface compared to hydrogels with a higher cross-link density. In a highly swollen hydrogel with less cross-linker, since a large amount of water is in the bulk phase of the gel, in order to minimise the interfacial tension at the surface, hydrophilic groups re-orientate towards the interior of the gel rather than remain on the surface, while the hydrophobic groups reorient

towards the surface hence contact angles for the R 90 gels are higher than that for gels which contain more cross-linker. However hydrogels with larger MBA content display reduced chain mobility, and enhanced polymer-polymer interactions due to an increase in the hydrophobic effect, hence the hydrophobic groups orientate towards the inner core while more hydrophilic groups and water remain on the surface consequently the contact angles of the R 10 gels are lower compared to R 90. The thermoresponsive behaviour of the hydrogels with a change in contact angle then can also be explained by the same concept, in that at 40 ℃, the hydrophobic isopropyl groups re-orientate at the surface and the contact angle increases, while at 20 ℃, some of the amide groups and water is also present at the gel-air interface due to an increase in hydrogen bonding and the contact angle is reduced (Zhang et al., 1995).

It can also be observed that the difference in contact angle at 20 ℃ and 40 ℃ decreases as the cross-link density increases. This can be attributed to restricted chain mobility at the gel-air interface with an increase in cross-link density; hence the difference in surface reorientation at both temperatures is smaller than for the gels with larger chain mobility.

4.4 Conclusions and recommendations

P(NIPAAm-*co*-MBA) hydrogels were successfully synthesised using the free radical polymerisation method and we have studied the thermoresponsive and physical properties of PNIPAAm hydrogels. To improve the response rate of PNIPAAm hydrogels, the cross-link density (R 90 to 10) and the use of mixed solvents were investigated. It was found that the swelling capacity of the PNIPAAm hydrogels decreased when the cross-link density increased from 90 to 10, however the de-swelling rate and pore density in the hydrogels increased with cross-link density. At 25 ℃ P(NIPAA m-*co*-MBA) hydrogels displayed relatively small pores, while at 37 ℃ porosity was completely lost. The LCST of the hydrogels was determined from micro DSC, and by dynamic oscillation shear rheology. The LCST was unaffected by the cross-link density. However the storage and loss modulus of the hydrogels was highly dependent on temperature and on the cross-link density for the gels. When NIPAAm was polymerised in mixed solvents, the LCST of PNIPAAm was maintained and superabsorbent heterogeneous polymer networks were created with very rapid response rates.

With respect to use of the P(NIPAAm-co-MBA) hydrogels for non-invasive cell culture, the following assessment was made:

- The porosity of the P(NIPAAm-*co*-MBA) hydrogels was largely lost at 37 °C which implies that during cell culture, the hydrogel surface will be similar to a 2D surface, and will not provide 3D structural support for the cells

- The pore size of the hydrogels in the hydrophilic state was also too small to enable release of 3D cell clusters, since if cells did penetrate into the bulk hydrogel during culture, cell release may be problematic

- De-swelling of standard PNIPAAm hydrogels in water is too slow and such a material will not be suitable for use in a robust system where a quick response is required

- Use of mixed solvents significantly improved the response rates of PNIPAAm hydrogels, but these gels displayed very poor stability. Effect of increasing the crosslink density on mixed-solvent gels could be the subject of future work

- The mechanical properties of the P(NIPAAm-*co*-MBA) hydrogels may be insufficient for use in a bioreactor with a perfusion system with a relatively high flow rate. It was observed that the R series gels underwent shear thinning with increases in frequency

- Difficulty with use of the bulk PNIPAAm polymer in e.g. a bioreactor where the entire scaffold will shrink and thereby influence the reactor flow rates etc.

- Use of bulk PNIPAAm hydrogel as a cell culture scaffold will be relatively expensive

Based on the considerations above, it was concluded that PNIPAAm bulk hydrogels may not be the ideal scaffold for cell culture, and cell culture studies was not pursued with this material. Application of a PNIPAAm layer onto a 3D preformed scaffold might prove more effective and hence was the subject of further investigation (**Chapter 5**).

4.5   References

Anseth KS, Bowman CN, Brannon-Peppas, L. 1996. Review Mechanical properties of hydrogels and their experimental determination, Biomaterials 17: 1647-1657.

Caykara T, Kiper S, Demirel G. 2006a. Network parameters and volume phase transition behaviour of poly(*N*-isopropylacrylamide) hydrogels. Journal of Applied Polymer Science 101:1756-1762.

Caykara T, Kiper S, Demirel G. 2006b. Thermosensitive poly(*N*-isopropylacrylamide-*co*-acrylamide hydrogels: Synthesis, swelling and interaction with ionic surfactants. European Polymer Journal 42:348-355.

Chetty AS, Kovács J, Vargha V, Mészáros A, Fekete J, Domján A. 2012.. A versatile characterisation of poly(*N*-isopropylacrylamide-*co*-N,N'-methylene-bis-acrylamide) hydrogels for composition, mechanical strength, and rheology, EXPRESS Polymer Letters, EPL-0003831, accepted: 26 June 2012.

DeRosa ME, DeRosa RL, Noni LM, Hendrick ES. 2007. Phase separation of Poly(*N*-isopropylacrylamide) solutions and gels using a near infrared fiber laser. Journal of Applied Polymer Science 105:2083–2090.

DeRossi D, Kajiwara K, Osada Y, Yamauchi A.(eds) 1991. Polymer gels - fundamental and biomedical applications. Plenum Press, New York pg 265.

Garbern JC, Hoffman AS, Stayton PS. 2010. Injectable pH and temperature-responsive poly(*N*-isopropylacrylamide-*co*-propylacrylic acid) copolymers for delivery of angiogenic growth factors. Biomacromolecules 11(7): 1833–1839.

Geever LM, Mi´nguez CM, Devine DM, Nugent MJD, Kennedy JE, Lyons JG, Hanley A, Devery S, Tomkins PT, Higginbotham CL. 2007. The synthesis, swelling behaviour and rheological properties of chemically cross-linked thermosensitive copolymers based on *N*-isopropylacrylamide. Journal of Material Science 42:4136–4148

Kara S, Okay O, Pekcan O. 2002. Real-time temperature and photon transmission measurements for monitoring phase separation during the formation of poly(*N*-isopropylacrylamide) gels. Journal of Applied Polymer Science 86:3589–3595.

Liang L, Shi M, Viswanathan VV, Peurrung LM, Young JS. 2000. Temperature-sensitive polypropylene membranes prepared by plasma polymerization. Journal of Membrane Science 177:97–108.

Lessard DG, Ousalem M, Zhu XX, Eisenberg A, Carreau PJ. 2003. Study of the phase transition of poly(N,N-diethylacrylamide) in water by rheology and dynamic light scattering. Journal of Polymer Science: Part B: Polymer Physics 41: 1627–1637.

Muniz EC, Geuskens G. 2001. Compressive elastic modulus of polyacrylamide hydrogels and semi-IPNs with poly(*N*-isopropylacrylamide). Macromolecules 34:4480-4484.

Riggs IP, Rodriguez F. 1967. Persulfate-initiated polymerisation of acrylamide. Journal of Polymer Science, Part A-1: Polymer. Chem. 5:3151-3165.

Takigawa T, Yamawaki T, Takahashi K, Masuda T. 1997. Change in Young's modulus of poly(*N*-isopropylacrylamide) gels by volume phase transition. Polymer Gels and Networks 5:585-589.

Yasuda T, Okuno T. 1994. Contact angle of water on polymer surfaces. Langmuir 10:2435-2439

Zhang J, Pelton R, Deng Y. 1995. Temperature-dependent contact angles of water on poly(*N*-isopropylacrylamide) gels. Langmuir 11:2301-2302.

Zhang X, Wu D, Chu CC. 2004. Synthesis, characterisation and controlled drug release of thermosensitive IPN-PNIPAAm hydrogels. Biomaterials 25:3793-3805.

Zhang X, Zhuo R, Yang Y. 2002a. Using mixed solvent to synthesize temperature sensitive poly(N-isopropylacrylamide) gel with rapid dynamics properties. Biomaterials 23:1313-1318.

Zhang XZ, Wu DQ, Chu CC. 2003. Effect of the cross-linking level on the properties of temperature-sensitive poly(*N*-isopropylacrylamide) hydrogels. Journal of Polymer Science: Part B: Polymer Physics 41:582–593

Zhang XZ, Xu XD, Cheng SX, and Zhuo RX. 2008. Strategies to improve the response rate of thermosensitive PNIPAAm hydrogels. Soft Matter 4:385–391.

Zhang XZ, Yang YY, Chung TS. 2002b. Effect of mixed solvents on characteristics of Poly(*N*-isopropylacrylamide) gel. Langmuir 18:2538-2542.